observed within 200 m zone. The area under 200 m radius from BOP is the zone of influence of blow-out. The gas blow-out site was inaccessible and satellite data alone facilitated in observing the vent temperature synoptically during the blow-out condition. In addition, multitemporal satellite data by virtue of repetitive coverage facilitated dynamic aspects of blow-out condition and the associated spatial changes resulting due to damage. Thus, satellite technology only could facilitate synoptic observation of such episodic events and could account spatially for the area of its influence.

1. Goward, S. N., Markham, B., Dye, D. G., Dulaney, W and Yang, J., *Remote Sens. Environ*, 1991, **35**, 257–277.
2. Rothery, D. A, Francis, P. W. and Wood, P. A, *J. Geophys. Res.*, 1988, **93**, 7993–8008.
3. Rothery, D. A, *Int. J. Remote Sens.*, 1989, **10**, 1423–1427.
4. Justice, C. O., Townshend, J. R. G., Holben, B. N. and Tucker, C. J., *Int. J. Remote Sens.*, 1985, **6**, 1271–1318.
5. Gupta, R. K. and Badarinath, K. V. S., *Int J. Remote Sens.*, 1993, **14**, 2907–2918.

ACKNOWLEDGEMENTS. We express our sincere gratitude to Prof. B. L. Deekshatulu, Director, NRSA, and Dr D. P. Rao, Associate Director, NRSA, for their encouragement. We are also grateful to Dr S. T. Chari, Group Director, Water Resources Group, NRSA, for the technical discussions.

Received 17 May 1995; revised accepted 28 August 1995

Oxygen linkages in neodymium heptamolybdate single crystals – An XPS study

Sushma Bhat, P. N. Kotru and K. S. Raju*

Department of Physics, Jammu University, Jammu 180 001, India
*Department of Crystallography and Biophysics, University of Madras, Guindy Campus, Madras 600 025, India

Single crystals of neodymium heptamolybdate ($Nd_2Mo_7O_{24} \cdot 27H_2O$) are grown in sodium metasilicate gel by the diffusion of neodymium nitrate (upper reactant) into the set gel impregnated with a mixture of molybdenum trioxide, ammonium hydroxide and concentrated nitric acid (lower reactant). Oscillation X-ray diffraction pattern shows that neodymium heptamolybdate is single-crystalline in nature, while infrared absorption spectrum establishes the presence of molybdate group and water of crystallization. X-ray photoelectron spectroscopic studies of neodymium heptamolybdate single crystals establish the presence of neodymium and molybdenum in their oxide states and the oxygens in the sample are shown to exist as (i) terminal oxygen (Mo=O), (ii) bridging oxygen (Mo–O–Nd) and (iii) oxygen of lattice water (H–O–H).

FERROELECTRIC and ferroelastic properties of rare-earth molybdates are of great interest in electro-optical and acousto-optical devices[1–3]. Barium molybdate tetragonal bipyramidal crystals are grown by the precipitation of alkaline-earth metal molybdate powders from neutral aqueous solutions[4]. Rare-earth molybdates, having the general formula $R_2(MoO_4)_3$, have been reported to be ferroelectric materials[5]. The growth of rare-earth molybdates (R = Pr, Nd, Sm, Eu, Tb and Dy) using the Czochralski technique has been studied by Brixner[6]. As this method involves elevated temperatures, thermal stresses released during the growth may make the crystals defective. Henisch and coworkers[7,8] have established the growth of crystals in gels and this method has been fully exploited in the case of calcium sulphate dihydrate single crystals[9–15]. Growth and characterization of rare-earth mixed single crystals of samarium barium molybdate have been reported by Isac and Ittyachen[16]. Studies on the growth of neodymium heptamolybdate (hereafter called NHM) single crystals in silica gels have been reported in the literature[17].

For the growth of NHM in gels in the test tube, acidified aqueous solution of sodium metasilicate (0.5 M, pH 5) is used as the reacting medium. The lower reactant (to be incorporated inside the gel before setting) is prepared as follows: 0.5 M molybdenum trioxide is completely dissolved in 15 N ammonium hydroxide using a magnetic stirrer, to which nitric acid (24 ml in 50 ml distilled water) is added. This lower reactant is mixed with the above gel and allowed to set undisturbed (gel age 96 h). On top of this set gel, as the upper reactant, a solution of 0.75 M neodymium nitrate is slowly added through the wall of the test tube, so as not to rupture the surface of the set gel. In about three weeks' time, platelets of NHM (of sizes 2 mm × 2 mm × 1 mm) appear below the thick white layer of the precipitate (of NHM) inside the gel.

The mechanism of chemical reactions leading to the formation of NHM is explained as follows:

$$MoO_3 + 2NH_4OH \rightarrow (NH_4)_2 MoO_4 + H_2O. \quad (1)$$

When acidified, we get

$$(MoO_4)^{2-} + H^+ \rightarrow HMoO_4^- , \quad (2)$$

$$HMoO_4^- + H^+ + 2H_2O \rightarrow Mo(OH)_6 , \quad (3)$$

$$Mo(OH)_6 + HMoO_4^- \rightarrow (HO)_5 MoOMoO_3 + H_2O, \quad (4)$$

$$(HO)_5 MoOMoO_3^- + HMoO_4^- \rightarrow (HO)_4 Mo(OMoO_3)_2^{2-} + H_2O, \quad (5)$$

*For correspondence

$$(HO)_4\,Mo(OMoO_3)_2^{2-} + 3HMoO_4^- \rightarrow (HO)\,Mo(OMoO_3)_5^{5-} + 3H_2O, \quad (6)$$

$$(HO)\,Mo(OMoO_3)_5^{5-} + HMoO_4^- \rightarrow Mo(OMoO_3)_6^{6-} + H_2O, \quad (7)$$

$$Mo(OMoO_3)_6^{6-} \rightarrow Mo_7O_{24}, \quad (8)$$

$$2Nd^{3+} + Mo_7O_{24}^{6-} \rightarrow Nd_2Mo_7O_{24}. \quad (9)$$

The oscillation X-ray diffraction (XRD) pattern (Figure 1) of NHM platelet was recorded in a Unicam camera with Cu K_α radiation ($\lambda = 1.5418$ Å). The revelation of well-defined Bragg reflections at specific (2θ) angles confirms that NHM is ordered, meaning single crystalline, in nature.

The IR absorption spectrum of NHM taken in KBr matrix confirms the presence of the water of crystallization by the well-defined broad peak at 3000–3600 cm^{-1} (relating to antisymmetric and symmetric OH sretchings) and a peak at 1630 cm^{-1} (relating to HOH bending). The presence of molybdate groups in NHM is also established by the revelation of a pronounced broad peak at 810 cm^{-1} relating to symmetric or antisymmetric stretching modes of vibration[18] and a peak at 325 cm^{-1} relating to symmetric bending modes of vibration[19].

It is worth mentioning, that in the present work, so far, neither XRD nor infrared (IR) absorption spectrum has been able to identify heavy elements like Mo and Nd unambiguously. Hence, it was thought worthwhile to take up the most sophisticated X-ray photoelectron spectroscopic (XPS) technique.

In XPS (more commonly known as ESCA), the identification of the elements incorporated in the sample is established from the binding energy (BE) values (eV) relating to the peaks of their respective elements, while the quantitative data are obtained from the peak heights or areas. The chemical states of the elements were identified from the exact positions and separations of the peaks, as well as from certain spectral contours. XPS studies were carried out on NHM single crystals in order to confirm the presence of heavy elements (Nd and Mo in the present case) besides their chemical states, which, consequently, sheds information on the linkages of the oxygens as well.

The XPS investigations of NHM were carried out at the Regional Sophisticated Instrumentation Centre, Indian Institute of Technology, Powai, Bombay, using a system VG scientific ESCALAB MK2 spectrometer (Al K_α source, photon energy 1486.6 eV) operated at 10 kV and 10 mA. The overall resolution of the system with an analyser pass of 50 eV is about 0.7 eV. The pressure in the analyser chamber was maintained below 10^{-9} torr.

In the present investigations, the BE (eV) scale (X-axis) was calibrated for C 1s (284.6 eV), which is due to the contribution of adventitious hydrocarbon from the laboratory environment or from the glove box.

The XPS peaks relating to Mo 3d states (Figure 2 *a*) are positioned at BEs of around 232.5 and 235.7 eV, with the separation of 3.2 eV strongly suggesting that Mo in NHM is in the oxide state (MoO_3). Similarly, the XPS peak relating to $3d_{5/2}$ state of Nd (Figure 2 *b*) in NHM has a BE of around 980 eV. This BE value confirms that Nd too is in its oxide state (Nd_2O_3) in the NHM sample, which is in good agreement with literature findings[20] on the structural characterization of

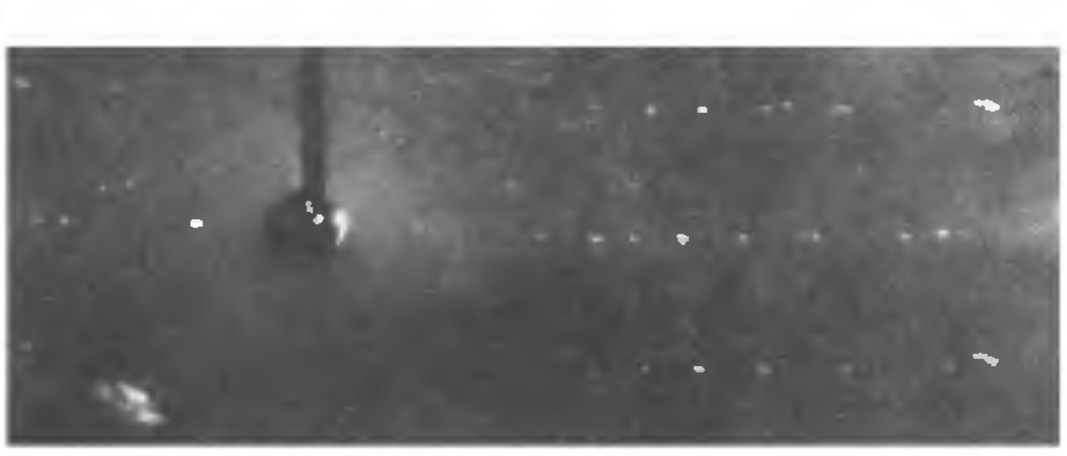

Figure 1. Oscillation XRD pattern of NHM.

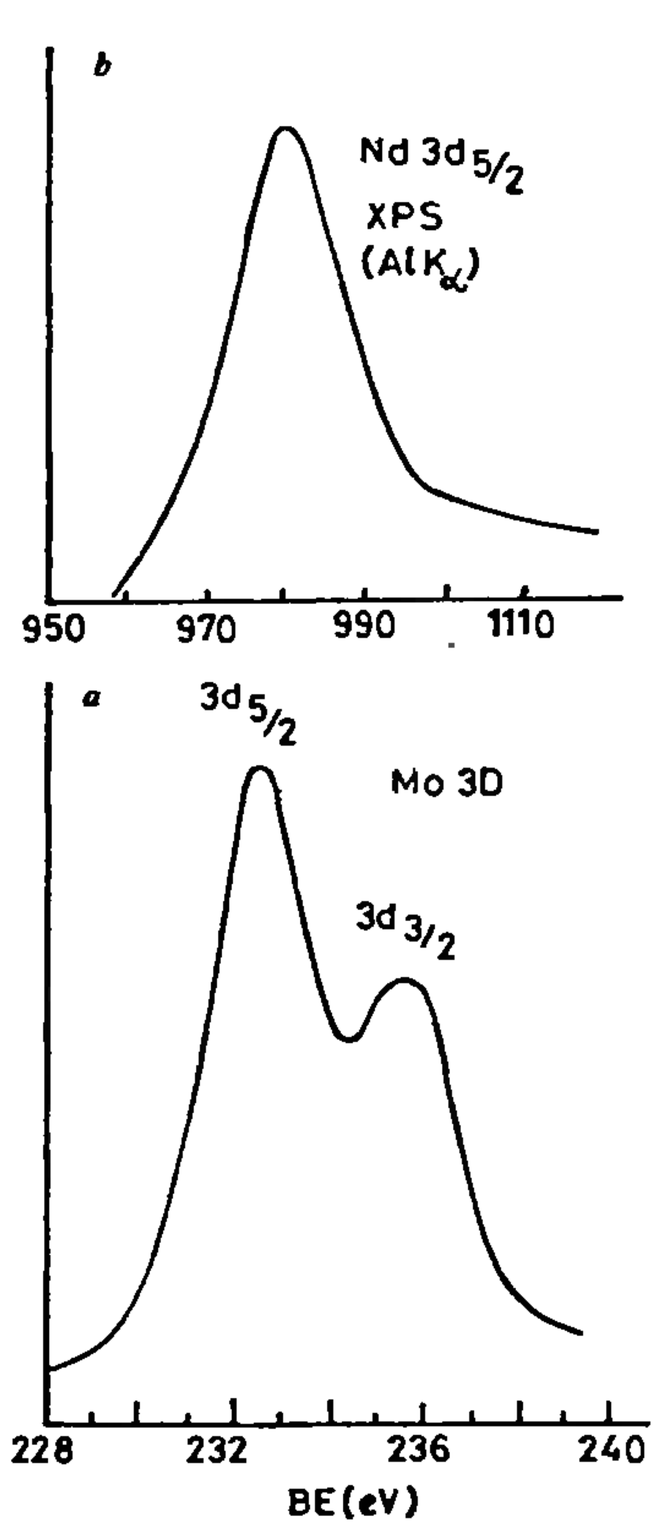

Figure 2. XPS peaks of (*a*) 3d levels of molybdenum and (*b*) $3d_{5/2}$ level of neodymium.

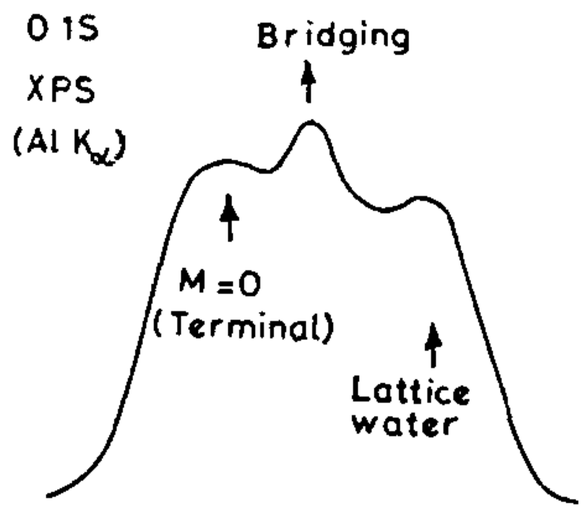

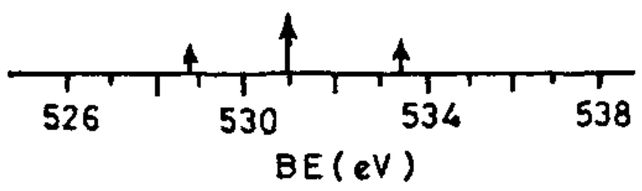

Figure 3. XPS peak of oxygen 1s.

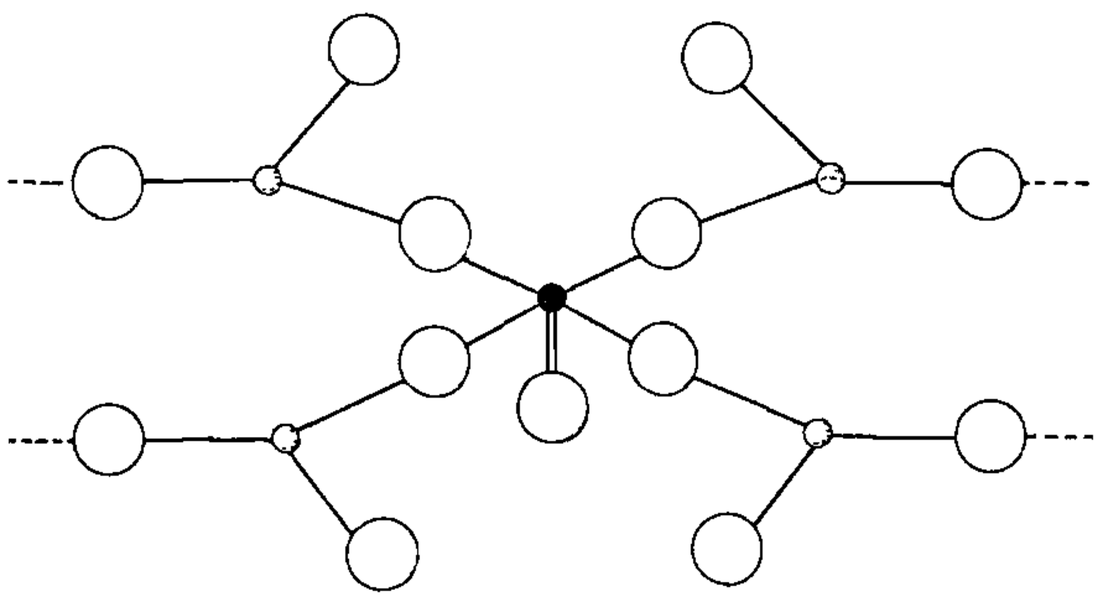

Figure 4. Schematic of oxygen coordinations in NHM: molybdenum (small dark circle), neodymium (small dashed circles) and oxygen (big blank circles).

gel-grown neodymium copper oxalate single crystals.

It is interesting to note that the XPS peak relating to O 1s (Figure 3) has a complex spectral contour and is a broad peak comprising of three peaks. These peaks relate to BEs around 528.8, 531 and 533.5 eV, respectively, giving the clue that oxygens in NHM have three different coordinations.

The incorporation of Mo, Nd and O in NHM has been confirmed by XPS (Figures 2 and 3) besides establishing the existence of Mo and Nd as their oxides (Figure 2 *a*, *b*). These conclusions are strongly supported by the binding energy values corresponding to XPS peaks of Mo(3d), Nd($3d_{5/2}$) and O(1s) (Figures 2 and 3), which are in excellent agreement with literature findings[21].

Attention is drawn to the fact that the chemical formula for NHM ($Nd_2Mo_7O_{24}$) as arrived at from the mechanism of reaction kinetics (eqs (1)–(9)) seems reasonable, as to be having the entities (Nd_2O_3) and $7(MoO_3)$, as supported by the XPS peaks of Nd and Mo in their oxide states (Figure 2). The possible oxygen linkages with MoO_3 and Nd_2O_3 in NHM are shown schematically in Figure 4. A careful examination of Figure 4 reveals that oxygens have two types of linkages, namely, terminal oxygen (Mo=O) and bridging oxygens (Mo–O–Nd). In order to account for the third entity, i.e. water of crystallization, the third peak in the complex spectral contour of XPS of O 1s (Figure 3) is attributed to the oxygen getting coordinated to the hydrogens of lattice water (H–O–H), whose presence is confirmed by the IR absorption spectrum of NHM. Thus, XPS studies throw light on the presence of Mo, Nd and O as well as on their chemical states, confirming the speculation of the entities of NHM as MoO_3, Nd_2O_3 and lattice water. Besides this, complex spectral contour of XPS peak of O 1s has been helpful in understanding the linkages of oxygens in NHM as well (Figure 4).

The heights and/or areas of XPS peaks, meaning their intensities, are measures of the quantities of the species present in the material[22]. It is clearly evident from Figure 3 that the intensity of O 1s relating to bridging oxygens is higher than that of terminal oxygens. Hence, it may be concluded that, from the viewpoint of structural aspects, the contribution of the bridging oxygens is more significant than that of the terminal oxygen in NHM.

1. Barkley, J. R., Brixner, L. H. and Horgan, E. M., IEEE Symp. on the Applications of Ferroelectrics, York Town Heights, New York, 1971.
2. Barkley, J. R., Brixner, L. H., Horgan, E. M. and Waring, R. K., *J. Ferroelec.*, 1972, **3**, 191–195.
3. Sapriel, J. and Vacher, R., *J. Appl. Phys.*, 1977, **48**, 1191–1194.
4. Pacter, A., *Krist. Tech.*, 1997, **12**, 729–732.
5. Borchordt, H. J. and Bierstedt, F. E., *Appl. Phys. Lett.*, 1966, **8**, 50–54.
6. Brixner, L. H., *J. Cryst. Growth*, 1973, **18**, 297–302.
7. Henisch, H. K., *Crystal Growth in Gels*, Pennsylvania State University Press, University Park, Pennsylvania, 1970.
8. Henisch, H. K., Dennis, J. and Hanoka, J. I., *J. Phys. Chem. Solids*, 1965, **26**, 493–500.
9. Raju, K. S., *Cryst. Res. Technol.*, 1983, **18**, 1277–1281.
10. Jayakumar, D. and Raju, K. S., *Bull. Mater. Sci*, 1983, **5**, 339–404.
11. Raju, K. S., *J. Mater. Sci. Lett.*, 1983, **2**, 705–709.
12. Raju, K. S., *J. Mater. Sci.*, 1981, **16**, 2512–2516
13. Raju, K. S., *J. Mater. Sci.*, 1985, **20**, 756–760.
14. Raju, K. S. and Pippel, E., *Phys. Stat. Solidi A*, 1984, **81**, K93–K95.
15. Raju, K. S., Godehardt, R., Hoppfe, J. and Pipple, E., *Cryst. Res. Technol.*, 1984, **19**, 1127–1131.
16. Isac, Jayakumari and Ittyachen, M. A., *Bull Mater. Sci*, 1992, **15**, 349–353.
17. Bhat, Sushma, Kotru, P. N. and Koul, M. L., *Mater. Sci. Engg B*, 1993, in press.
18. Busy, R. H. and Keller, O. L., Jr, *J. Chem. Phys*, 1964, **41**, 215–225.
19. Clark, G. M and Doyle, W. P., *Spectrochim. Acta*, 1966, **22**, 1441–1447.
20. Raju, K. S., Krishna, K. N, Isac, Jayakumari and Ittyachen, M A,

Bull Mater Sci., 1994, **17**, 1447–1455.
21 Wagner, C D., Riggs, W. M., Davis, L. E., Moulder, J. F. and Mullenberg, J E (eds), *Handbook of X-ray Photoelectron Spectroscopy*, Perkin Elmer, Physical Electronics Division, Minnesota, 1978
22. Riggs, W. M and Parker, M. J., in *Methods of Surface Analysis* (ed Czanderna, A. W.), Elsevier, Amsterdam, 1975, Chap. 4, p. 108.

ACKNOWLEDGEMENTS We thank the Regional Sophisticated Instrumentation Centre, Indian Institute of Technology, Powai, Bombay, for the ESCA facility. KSR thanks Prof. B. Viswanathan, Department of Chemistry, Indian Institute of Technology, Madras, for stimulating discussions.

Received 27 March 1995; revised accepted 5 June 1995

Tectonic evolution of the Central Gujarat plain, western India

D. M. Maurya, L. S. Chamyal and S. S. Merh

Department of Geology, Faculty of Science, M S. University of Baroda, Baroda 390 002, India

The Quaternary basin of the Gujarat plain is formed due to the reactivation of Tertiary basement faults. The uplift as a horst of the Aravalli in the east and the Saurashtra peninsula in the west, comprising a culminating event of the post-Mesozoic rifting of the western continental margin, resulted in the Quaternary basin which was later filled up by alluvial sediments. The basin that received the fluvial sediments marked the end phase of the Cambay graben subsidence that was initiated in the Paleocene. The nature of variation in thickness of the Quaternary sediments in its different segments indicates that the basin comprised a series of horsts and grabens. Whereas the Early Quaternary tectonism gave rise to the differential basement topography, the tectonic events of the Late Quaternary were responsible for the present landscape development in Central Gujarat.

THE 300–800 m thickness of Quaternary fluvial and aeolian sediments resting upon the Tertiary rocks of the Cambay basin is the consequence of reactivation of pre-Quaternary basement faults. The Quaternary basin is delimited by marginal faults in the west and east. To the SE lies the Narmada–Son Lineament, and in the NE is the Aravalli horst (Figure 1). The basin comprises several fault-bound structural blocks[1] which continue up to Moho boundary[2]. The Gujarat Quaternary sediments have been studied by several workers (Allchin *et al.*[3], Chamyal[4], Chamyal and Merh[5], Merh and Chamyal[6] and Pant and Chamyal[7]); their emphasis, however, was mainly on the processes and agents of deposition, and on the paleoclimatic variations recorded in sediments. Recent work has demonstrated that successive tectonic events in the Gujarat region since Cretaceous[8] have also controlled the pattern of sedimentation and nature of the sediment body. The Cambay and Narmada basins, according to Biswas[8] opened up as a result of the counterclockwise rotation accompanying drift of the Indian plate.

The Gujarat plains, in the light of the overall Cambay basin tectonics, point to an important role played by differential movements along numerous structural lineaments in controlling the process of filling up of the Quaternary basin and sculpturing the present-day landscape. The movements along tectonic lineaments at various scales are significantly reflected in (i) the disruption of an ancient superfluvial system and its replacement by the existing drainage[9], (ii) development of ravines along various river courses indicating post-depositional fracturing, (iii) differential altitudes of river terraces, (iv) capturing of rivers (e.g. Rupen by Sabarmati, Orsang by Narmada), (v) differential uplifts along most major rivers giving rise to a distinct northward tilting of the respective left banks, and (vi) progressively increasing subsidence from south to north[10].

We have for the first time attempted to interpret the role of tectonics in the evolution of the Quaternary basin and its subsequent filling. Obviously, the Quaternary sedimentation is found to have been controlled by the same tectonic features which were responsible for the deposition of the Tertiaries. With the withdrawal of the Tertiary sea in this part, marine processes were replaced by fluvial sedimentation, marking the onset of the nonmarine continental depositional cycles. The marine sediments of Upper Tertiary show a transition[11] changing over to a period dominantly of fluvial sedimentation during the Quaternary.

The basin that received Quaternary sediments, obviously, comprised the more or less filled up Tertiary Cambay basin and marked the culminating phase of the Cambay and Narmada graben tectonics, though the tectonism preceding, during and post-dating the continental deposition was an integral part of the Cambay basin tectonism. ONGC investigations have adequately shown that the Cambay basin formed during Paleocene subsided episodically with varying rates and finally during Quaternary the rate of subsidence slowed down. It is however, not unlikely that the Quaternary basin experienced considerable reactivation of the pre-existing faults. These faults were an integral part of the Cambay basin rift phenomenon. It is possible that the advent of Pleistocene witnessed a renewal of tectonic activity and triggering of a new cycle of subsidence. This neotectonism coincided with the uplift of Aravalli in the east and northeast[12]. An uplift of the order of 300 m of the Aravalli has been envisaged by Ahmad[13] during Quaternary. To